Research Article

Valeria Bacchelli, Dario Pierotti, Stefano Micheletti* and Simona Perotto

Parameter identification for the linear wave equation with Robin boundary condition

https://doi.org/10.1515/jiip-2017-0093
Received June 14, 2017; revised March 29, 2018; accepted March 29, 2018

Abstract: We consider an initial-boundary value problem for the classical linear wave equation, where mixed boundary conditions of Dirichlet and Neumann/Robin type are enforced at the endpoints of a bounded interval. First, by a careful application of the method of characteristics, we derive a closed-form representation of the solution for an impulsive Dirichlet data at the left endpoint, and valid for either a Neumann or a Robin data at the right endpoint. Then we devise a reconstruction procedure for identifying both the interval length and the Robin parameter. We provide a corresponding stability result and verify numerically its performance moving from a finite element discretization.

Keywords: Wave equation, method of characteristics, solutions in closed form, parameter estimation, stability analysis, finite element method, Newmark method

MSC 2010: 35L05, 35L20, 35C05, 35R30, 65M60, 65L09

Dedicated to Fausto

1 Introduction

Let us consider the following mixed boundary value problem for the wave equation:

$$\begin{cases} u_{xx} - u_{tt} = 0, & 0 < x < b,\ t > 0, \\ u(x,0) = 0, & 0 < x < b, \\ u_t(x,0) = 0, & 0 < x < b, \\ u(0,t) = h(t), & t \geq 0, \\ u_x(b,t) + \gamma u(b,t) = 0, & t \geq 0, \end{cases} \tag{1.1}$$

where $b > 0$, $\gamma \geq 0$ and $h(t)$ is a $\mathcal{C}^1$ function in $[0, +\infty)$ such that $h(0) = 0$ are assigned data. The above system, though pretty simple, actually models some physical problems of interest in engineering applications. For instance, the unknown function $u(x, t)$ describes the transverse vibrations of a string of finite length, with respect to the horizontal rest configuration, with vertical component of the tension given by $u_x(x, t)$. In this context, Dirichlet, Neumann and Robin boundary conditions have a direct physical interpretation. In particular, a null Neumann data, $u_x(b, t) = 0$, is associated with a free transverse motion, i.e., no external transverse force acts on this end; a homogeneous Robin condition, $u_x(b, t) + \gamma u(b, t) = 0$, represents a linearly restora-

Valeria Bacchelli, Dario Pierotti, Dipartimento di Matematica, Politecnico di Milano, Piazza L. da Vinci 32, 20133, Milano, Italy, e-mail: valeria.bacchelli@polimi.it, dario.pierotti@polimi.it
***Corresponding author: Stefano Micheletti,** MOX, Dipartimento di Matematica, Politecnico di Milano, Piazza L. da Vinci 32, 20133, Milano, Italy, e-mail: stefano.micheletti@polimi.it
Simona Perotto, MOX, Dipartimento di Matematica, Politecnico di Milano, Piazza L. da Vinci 32, 20133, Milano, Italy, e-mail: simona.perotto@polimi.it

tive transverse force, that is, the end is transversally restrained, but elastically rather than rigidly [12]. For this reason, this last condition is often referred to as elastic.

Another relevant application of the wave equation is in acoustics, where u is the velocity potential associated with the propagation of a pressure wave in a carrier medium [1]. The Dirichlet boundary condition on a certain surface, for a complex amplitude pressure, is applied when the material of the surface has very low acoustic impedance compared to that of the medium. In this case, the surface is called sound soft. Vice versa, when the surface material has much higher acoustic impedance than the one of the host medium, a Neumann boundary condition holds, and the surface is called sound hard. The Robin (or impedance) boundary condition models finite acoustic impedance, γ being proportional to the admittance of the surface.

We suppose that the boundary, $x = b$, is unknown and inaccessible, whereas $x = 0$ is accessible for input and output measurements. Then we deal with the inverse problem of determining b and γ, provided additional measurements $u_x(0, t)$ are known for t in a bounded interval $(0, t_f)$.

An analogous problem was considered in spatial dimension $d \geq 2$ by Isakov [7], assuming that the unknown boundary Γ is a closed *polygonal surface*. Isakov proved that an additional measurement of the normal derivative on the known part of the boundary for large enough t_f uniquely determines Γ and γ. Moreover, inverse problems involving a Robin condition in a *parabolic* equation were considered by Bacchelli, Di Cristo, Sinchich and Vessella [2]. They prove that two pairs of measurements guarantee uniqueness and stability of both Γ and γ. In the context of hyperbolic problems, although addressing different identification problems, it is worth mentioning the following works: In [13], the wave equation is considered where the spatial operator is in conservation form $(K(x)u_x)_x$ and the problem is set on the half line $x > 0$. An inverse problem for the identification of the coefficient $K(x)$ is proposed, based on the boundary impulse response, i.e., by measuring the function $u(x, 0) = f(t)$ associated with the Neumann boundary condition $u_x(0, t) = \delta(t)$. A similar problem in addressed in [9], where the inverse medium problem associated with the reconstruction of the heterogeneous material profile of a semi-infinite layered soil medium, directly in the time domain, is studied. The method is based on the complete waveform response of the medium to a forcing Neumann boundary condition on the surface. The inversion process relies on a partial differential equation constrained optimization approach, supplemented with a time-dependent regularization scheme. An absorbing boundary condition is enforced at the bottom of the domain, at a certain depth, to take into account the artificial truncation of the spatial domain. Moreover, for the case when there is no homogeneous bottom layer, or its precise location is not a priori known, Na and Kallivokas [9] propose two iterative schemes to identify the domain depth. A force identification problem for the wave equation is studied in [8], where the space-dependent part of the source term is recovered from measurements of the final or time-average displacement of the wave. Finally, in [5], a nonlinear inverse coefficient problem for the wave equation is investigated. Namely, the nonlinear reconstruction of the space-dependent potential (the coefficient $Q_0(x)$ of u) and/or of the damping (the coefficient $Q_1(x)$ of u_t) from Cauchy data boundary measurements of the solution and of its normal derivative are studied both theoretically in $\mathbb{R}^n$ for $n = 1, 2, 3$, and numerically in one dimension.

In this paper, we uniquely identify the pair (b, γ) by evaluating the output flux $u_x(0, t)$ of the solution generated by an *impulsive Dirichlet data* $h(t)$ for a sufficiently large time interval. We stress that no a priori bound is required on γ, so that we include the limit case $\gamma = 0$ of the Neumann problem. Moreover, only a lower bound $b \geq b_0 > 0$ is assumed on the length of the unknown interval. By adding a further upper bound on γ, we also provide a stability estimate (see Section 3.1).

A key point is the determination of the closed-form solution to (1.1), at least up to a definite time, but in principle extendable to any larger time. This is carried out by a careful application of the method of characteristics, which we exploit to build the solution in space-time triangular domains. Clearly, the domain of dependence of u at a given space-time point, say $(\bar{x}, \bar{t})$, is the interval $[\bar{x} - \bar{t}, \bar{x} + \bar{t}]$, whose width increases with $\bar{t}$, making the procedure more involved.

We remark that a closed-form solution of (1.1) was provided in [11], for the case of non-homogeneous boundary conditions. In this paper, we provide the explicit construction based on the method of characteristics both for the sake of completeness and with a view to possible generalizations of our method for identifying b and γ to the case of a time dependent Robin coefficient $\gamma(t)$ (see Remark 2.2 and Section 5),

not treated in [11], and to the case of an inhomogeneous Robin boundary condition (see Remark 2.3 and Section 5).

Then the performance of the identification procedure is tested numerically. We devise an algorithm which takes into account the unavoidable approximations and smoothing effects introduced by the numerical discretization. In particular, the wave equation is dealt with a Galerkin finite element method with polynomial approximation of arbitrary degree for the spatial variable, and a Newmark method to advance in time. The impulsive Dirichlet data is approximated by a Gaussian function of unit area and with a very small variance. The overall scheme is unconditionally stable (with a proper selection of the parameters in the Newmark method), and we show that one can obtain a very accurate reconstruction of the physical parameters. Actually, very small space and time discretization steps are required to describe the sharp Gaussian profile and to reduce the dispersion error of the method.

The paper is organized as follows: In Section 2, we exploit the method of characteristics to obtain an explicit representation (for some bounded time interval) of the solution to (1.1) with $h(t) = \delta(t - t_0)$, $t_0 > 0$. In Section 3, we first discuss the motivations leading to the proposed reconstruction procedure based on a measurement of the output flux on a time interval; then we define a function $g(T)$ by a suitable weighted integral on $(0, T)$ of the output flux $u_x(0, t)$ and we show that the study of g allows us to uniquely determine the pair (b, γ) (see Proposition 3.2). Finally, the stability is discussed by defining an appropriate notion of distance between a pair of such functions g. In Section 4, we introduce the numerical algorithm employed to assess the robustness and accuracy of the identification procedure. Some conclusions and possible generalizations are discussed in Section 5.

2 A representation formula of the solution

As it is known, problem (1.1) has a unique classical solution $u \in \mathcal{C}^2((0, b) \times (0, +\infty)) \cap \mathcal{C}^1([0, b] \times (0, +\infty))$ (see [6]). We provide here a closed-form representation of the solution on a specific bounded time interval.

Proposition 2.1. *A representation $u_x(0, t)$ of the flux,* valid in the interval $0 < t < 3b$, *is provided by*

$$u_x(0,t) = -h'(t) + \begin{cases} 0, & 0 < t < 2b, \\ 2h'(t-2b) - 4\gamma h(t-2b) + 4\gamma^2 e^{-\gamma(t-2b)} \displaystyle\int_0^{t-2b} e^{\gamma s} h(s)\, ds, & 2b < t < 3b. \end{cases} \tag{2.1}$$

Proof. This proof is based on a repeated application of the method of characteristics [3]. To this end, it is enough to obtain an explicit expression for the solution in the triangles T_0 and T_2 in Figure 1. As it should be clear from this picture, for the evaluation of the solution in T_2 we need to compute the solution also in T_1, where the influence of the Robin boundary condition first appears. Thus we divide the proof into three steps, by processing each triangle in turn.

Solution in T_0. We observe that the solution u is vanishing for $0 \le x \le b$ and $0 \le t \le x$, while in the triangle T_0 defined by

$$T_0 := \{0 \le x \le b : x \le t \le 2b - x\}$$

we simply have $u(x, t) = h(t - x)$. Hence,

$$u_x(0, t) = -h'(t) \quad \text{for } 0 \le t < 2b.$$

Solution in T_1. We now represent the solution $u(x, t)$ in the triangle

$$T_1 := \left\{\frac{b}{2} \le x \le b : 2b - x \le t \le x + b\right\}.$$

Then, thanks to the d'Alembert formula, we write the solution in T_1 in the form

$$u(x,t) = \frac{1}{2}\phi(x - t + b) + \frac{1}{2}\phi(x + t - b) + \frac{1}{2}\int_{x-t+b}^{x+t-b} \psi(s)\, ds, \tag{2.2}$$

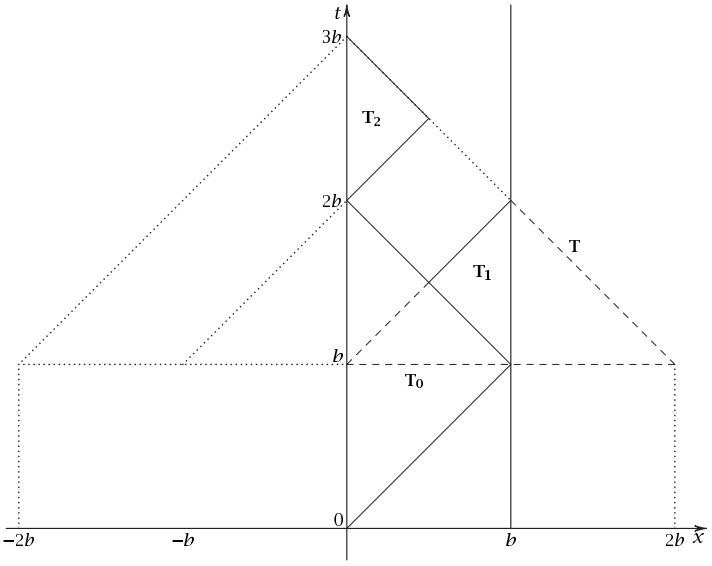

Figure 1: Graphic representation of the method of characteristics.

where ϕ, ψ are the Cauchy data at $t = b$, which depend on the solution at previous times. Clearly, in the interval $0 \le x \le b$ we have $\phi(x) = h(b - x)$ and $\psi(x) = h'(b - x)$. Additionally, to define (2.2) for $(x, t) \in T_1$ it is necessary to specify the data ϕ, ψ in the whole interval $0 \le x \le 2b$. This can be accomplished by exploiting the Robin boundary condition.

For this purpose, we rewrite (2.2) as

$$u(x,t) = \frac{1}{2}h(t-x) + \frac{1}{2}\phi(x+t-b) + \frac{1}{2}\int_{x-t+b}^{b} h'(b-s)\,ds + \frac{1}{2}\int_{b}^{x+t-b} \psi(s)\,ds.$$

By explicitly integrating the third term, and since $h(0) = 0$, we have

$$u(x,t) = h(t-x) + H(t+x-b), \tag{2.3}$$

where

$$H(\xi) = \frac{1}{2}\phi(\xi) + \frac{1}{2}\int_{b}^{\xi} \psi(s)\,ds, \quad b \le \xi \le 2b.$$

We now determine the unknown function H by imposing the boundary condition $u_x(b,t) + \gamma u(b,t) = 0$. We obtain the Cauchy problem

$$\begin{cases} H'(t) + \gamma H(t) = h'(t-b) - \gamma h(t-b), & t > b, \\ H(b) = \frac{1}{2}\phi(b) = \frac{1}{2}h(0) = 0. \end{cases} \tag{2.4}$$

The solution to this problem is given by

$$H(t) = h(t-b) - 2\gamma e^{-\gamma(t-b)} \int_{0}^{t-b} e^{\gamma s} h(s)\,ds = h(t-b) - 2\gamma \tilde{h}(t-b),$$

where

$$\tilde{h}(\xi) := e^{-\gamma\xi} \int_{0}^{\xi} e^{\gamma s} h(s)\,ds. \tag{2.5}$$

Note that $\tilde{h}' = h - \gamma\tilde{h}$. By plugging the expression of H into (2.3), we obtain

$$u(x,t) = h(t-x) + h(t+x-2b) - 2\gamma\tilde{h}(t+x-2b) \tag{2.6}$$

for $(x,t) \in T_1$.

We now determine the functions ϕ, ψ in (2.2). Let us consider the triangle

$$T := \{b \le t \le 2b : t - b \le x \le 3b - t\},$$

which includes T_1, a part of T_0 and a part of the half-plane $x > b$ (see Figure 1). By (2.6), and since $u(x,t) = h(t-x)$ in T_0, it can be easily checked that u coincides with the solution (still denoted by u) of the wave equation in T with Cauchy data at $t = b$ given by

$$u(x,b) = \begin{cases} h(b-x), & 0 \le x \le b, \\ h(x-b) - 2\gamma\tilde{h}(x-b), & b \le x \le 2b, \end{cases} \tag{2.7}$$

and

$$u_t(x,b) = \begin{cases} h'(b-x), & 0 \le x \le b, \\ h'(x-b) - 2\gamma h(x-b) + 2\gamma^2\tilde{h}(x-b), & b \le x \le 2b. \end{cases} \tag{2.8}$$

By comparison with (2.2), it follows that the right-hand sides of (2.7) and (2.8) are the required functions ϕ, ψ in $b \le x \le 2b$.

Solution in T_2. We can now go further by evaluating the solution in the upper triangle

$$T_2 := \left\{0 \le x \le \frac{b}{2} : 2b + x \le t \le 3b - x\right\}.$$

To this end, we still employ the d'Alembert formula (2.2) to represent the solution $u(x,t)$. However, since $(x,t) \in T_2$, the initial values at $t = b$ have to be defined in the larger interval $-2b \le x \le 2b$. Using (2.7) and (2.8) and since, for $(x,t) \in T_2$, one has $-2b \le x - t + b \le -b$ and $b \le x + t - b \le 2b$, it holds

$$u(x,t) = K(x-t+b) + \frac{1}{2}\left[h(x+t-2b) - 2\gamma\tilde{h}(x+t-2b)\right] + \frac{1}{2}\int_0^b h'(b-s)\,ds$$
$$+ \frac{1}{2}\int_b^{x+t-b} \left[h'(s-b) - 2\gamma h(s-b) + 2\gamma^2\tilde{h}(s-b)\right] ds,$$

where

$$K(\xi) := \frac{1}{2}\phi(\xi) + \frac{1}{2}\int_\xi^0 \psi(s)\,ds, \quad -2b \le \xi \le 0.$$

By explicit integration of the terms containing h', we obtain

$$u(x,t) = K(x-t+b) + \frac{1}{2}h(b) + h(x+t-2b) - \gamma\tilde{h}(x+t-2b) - \gamma\int_0^{x+t-2b} h(s)\,ds + \gamma^2\int_0^{x+t-2b} \tilde{h}(s)\,ds. \tag{2.9}$$

To determine the unknown function K, we enforce the Dirichlet condition $u(0,t) = h(t)$ for $t \ge b$, so that

$$K(b-t) + \frac{1}{2}h(b) + h(t-2b) - \gamma\tilde{h}(t-2b) - \gamma\int_0^{t-2b} h(s)\,ds + \gamma^2\int_0^{t-2b} \tilde{h}(s)\,ds = h(t).$$

By solving for K and by replacing t by $t - x$, we have

$$K(x-t+b) = h(t-x) - \frac{1}{2}h(b) - h(t-x-2b) + \gamma\tilde{h}(t-x-2b) + \gamma\int_0^{t-x-2b} h(s)\,ds - \gamma^2\int_0^{t-x-2b} \tilde{h}(s)\,ds.$$

Finally, using this expression in (2.9), we obtain

$$u(x,t) = h(t-x) + h(x+t-2b) - h(t-x-2b) - 2\gamma[\tilde{h}(x+t-2b) - \tilde{h}(t-x-2b)],$$

where $\tilde{h}$ is given by (2.5), with $0 \le x \le \frac{b}{2}$ and $2b + x \le t \le 3b - x$. Hence, by recalling that $\tilde{h}' = h - \gamma\tilde{h}$, we obtain

$$u_x(0,t) = -h'(t) + 2h'(t-2b) - 4\gamma h(t-2b) + 4\gamma^2\tilde{h}(t-2b), \quad 2b < t < 3b,$$

so that (2.1) is proved. □

Remark 2.2. We can easily extend (2.1) to the case of a time dependent $\gamma = \gamma(t)$. In fact, the main difference with respect to the proof of Proposition 2.1 is the Cauchy problem (2.4), which still can be solved by explicit integration. Then, by elementary calculations and following the same steps as above, we obtain the representation formula

$$u_x(0,t) = -h'(t) + \begin{cases} 0, & 0 < t < 2b, \\ 2h'(t-2b) - 4\gamma(t-b)h(t-2b) + 4\gamma(t-b)\tilde{h}_\gamma(t-b), & 2b < t < 3b, \end{cases} \tag{2.10}$$

where

$$\tilde{h}_\gamma(\xi) := e^{-\Gamma(\xi)} \int_b^\xi e^{\Gamma(s)}\gamma(s)h(s-b)\,ds, \qquad \Gamma(\xi) := \int_b^\xi \gamma(s)\,ds.$$

Remark 2.3. When dealing with an inhomogeneous Robin condition, by linearity, we can write the solution in the form $u(x,t) + w(x,t)$, where u is the solution to the original problem (1.1) and w solves the wave equation with the boundary conditions: $w(0,t) = 0$ and $w_x(b,t) + \gamma w(b,t) = f(t)$. We assume that $f(t)$ is defined for $t \ge 0$ and is locally integrable.

It can be checked that, for $0 \le x \le b$,

$$w(x,t) = \begin{cases} 0, & 0 \le t \le b - x, \\ \tilde{f}(t+x-b), & b - x \le t \le b + x, \\ \tilde{f}(t+x-b) - \tilde{f}(t-x-b), & b + x \le t \le 3b - x, \end{cases}$$

where

$$\tilde{f}(\xi) := e^{-\gamma\xi} \int_0^\xi e^{\gamma s} f(s)\,ds.$$

Note that $\tilde{f}(0) = 0$ and $\tilde{f}'(\xi) = f(\xi) - \gamma\tilde{f}(\xi)$.

Now, the representation formula (2.1) is replaced by

$$u_x(0,t) + w_x(0,t) = -h'(t) + \begin{cases} 0, & 0 < t < b, \\ 2f(t-b) - 2\gamma\tilde{f}(t-b), & b < t < 2b, \\ 2f(t-b) - 2\gamma\tilde{f}(t-b) + 2h'(t-2b) - 4\gamma h(t-2b) & \\ \quad + 4\gamma^2 e^{-\gamma(t-2b)} \int_0^{t-2b} e^{\gamma s} h(s)\,ds, & 2b < t < 3b. \end{cases}$$

3 The inverse problem

Suppose $0 < b_0 \le b$, $\gamma \ge 0$. The inverse problem of interest consists in determining uniquely b and γ, by choosing a suitable input $h(t)$ and by measuring the output flux $u_x(0,t)$, namely we aim to recover the unknown pair of constants (b,γ) by measuring the flux at $x = 0$ generated by an impulse at time t_0.

By inserting in the representation (2.1) the impulse

$$h(t) = \delta(t - t_0), \tag{3.1}$$

where $t_0 > 0$ is a suitable small time, we have

$$u_x(0, t) = -\delta'(t - t_0) + 2\delta'(t - (2b + t_0)) - 4\gamma\delta(t - (2b + t_0)) + 4\gamma^2 e^{-\gamma(t-(2b+t_0))}\mathbf{1}_{(2b+t_0,3b)}(t), \tag{3.2}$$

where $0 < t < 3b$ and $\mathbf{1}_{(a,b)}$ denotes the indicator function of the interval (a, b).

Clearly, equation (3.2) holds in the distribution sense, and can be obtained as the limit of (2.1) for a sequence $\{h_n(t)\}$ of boundary data such that $h_n(t) \to \delta(t - t_0)$ (e.g., a sequence of Gaussian functions centered at t_0). In this case, after multiplying the first equation of (1.1) by $\phi \in \mathcal{C}^2(Q_T)$, with $Q_T := [0, b] \times [0, T]$, integrating by parts and taking the limit above, we have that u is a weak solution to problem (1.1) in the following sense: u is a continuous functional on $\mathcal{C}(Q_T)$ (i.e., a Radon measure) for every $T > t_0$, satisfying

$$\int_0^b \int_0^T u(x, t)[\phi_{xx}(x, t) - \phi_{tt}(x, t)]\, dx\, dt + \int_0^T \delta(t - t_0)\phi_x(0, t)\, dt = 0 \tag{3.3}$$

for every $\phi \in \mathcal{C}^2(Q_T)$ such that

$$\begin{aligned} &\phi(0, t) = 0, \quad \phi_x(b, t) + \gamma\phi(b, t) = 0, && 0 \le t \le T, \\ &\phi(x, T) = 0, \qquad\qquad \phi_t(x, T) = 0, && 0 \le x \le b. \end{aligned}$$

Uniqueness of the above weak solution can also be checked. For this, let u_1, u_2 be two solutions of (3.3) in the dual space $\mathcal{C}(Q_T)'$ and let $\varphi \in \mathcal{C}(Q_T)$ be arbitrary. By classical results, there exists a unique $\phi \in \mathcal{C}^2(Q_T)$ satisfying $\phi_{xx}(x, t) - \phi_{tt}(x, t) = \varphi(x, t)$ and the above boundary conditions. Then

$$\int_0^b \int_0^T (u_1(x, t) - u_2(x, t))\varphi(x, t)\, dx\, dt = \int_0^b \int_0^T (u_1(x, t) - u_2(x, t))[\phi_{xx}(x, t) - \phi_{tt}(x, t)]\, dx\, dt = 0,$$

so that $u_1 = u_2$ by the arbitrariness of φ.

Remark 3.1. By inspection of the right-hand side of (3.2), we see that for $t > t_0$ (i.e., after shooting the impulse at the accessible boundary) the output flux consists of two "singular" terms at $t = 2b + t_0$, followed by an exponentially decreasing term. Then, by assuming some a priori upper bound $b \le \bar{b}$, one could try to recover the pair (b, γ) by measuring $u_x(0, t)$ at two distinct times t_1 and t_2 larger than $2\bar{b} + t_0$, and by using (3.2) when $2\bar{b} + t_0 < 3b_0$, or vice versa its suitable extension provided in [11]. Nevertheless, if no reasonable upper bound on b is available, one is forced to measure the output flux on a suitable interval of time in order to detect the perturbation generated by the initial impulse. Besides, even if such an upper bound is known, it turns out that the identification of (b, γ) with two measurements of the flux at distinct times becomes unstable for $\gamma \to 0$. In fact, in the limit case of the Neumann condition at b (i.e., $\gamma = 0$), the representation formula (3.2) shows that $u_x(0, t)$ is concentrated at the unknown time $t = 2b + t_0$ (more generally, at $t = 2nb + t_0$, $n = 1, 2, \ldots$), so that the identification of b by measuring $u_x(0, t)$ at a single time does not seem feasible.

We will take as observable output boundary data some weighted integral of (3.2) with test function *supported in the interval* $[0, 3b)$. The presence of the derivatives of the delta function in (3.2) leads to using $\mathcal{C}^1$ weight functions (i.e., we can not simply integrate the output flux on some interval $[0, T] \subset [0, 3b)$). However, piecewise smooth, continuous functions can be chosen too. Thus, for every $T \ge \frac{b_0}{2}$, we consider the continuous, piecewise linear function

$$\varphi_T(t) := \begin{cases} 1, & 0 \le t \le T - \dfrac{b_0}{2}, \\ \dfrac{2}{b_0}(T - t), & T - \dfrac{b_0}{2} \le t \le T, \\ 0, & t \ge T. \end{cases} \tag{3.4}$$

Assume further that $t_0 < \frac{b_0}{2}$ and $t_0 + \frac{b_0}{2} \le T < 3b$. Then we define

$$g(T) := \int_0^T u_x(0,t)\varphi_T(t)\,dt, \tag{3.5}$$

with $u_x(0,t)$ as in (3.2). Note that the integral can be extended to the interval $[0, 3b)$ by exploiting the bounded support of φ_T. In practice, the function g represents the so-called observed data.

By the properties of the delta function and of its derivative, we obtain

$$g(T) = \begin{cases} 0 & \text{for } t_0 + \dfrac{b_0}{2} \le T < 2b + t_0, \\ \dfrac{4}{b_0} - \dfrac{8\gamma}{b_0}(T - (2b + t_0)) + \dfrac{8\gamma^2}{b_0}\displaystyle\int_{2b+t_0}^{T} s(t)(T-t)\,dt & \text{for } 2b + t_0 < T < 2b + t_0 + \dfrac{b_0}{2}, \\ -4\gamma + 4\gamma^2 \displaystyle\int_{2b+t_0}^{T-\frac{b_0}{2}} s(t)\,dt + \dfrac{8\gamma^2}{b_0}\displaystyle\int_{T-\frac{b_0}{2}}^{T} s(t)(T-t)\,dt & \text{for } 2b + t_0 + \dfrac{b_0}{2} < T \le 3b, \end{cases}$$

where, to simplify notation, we set $s(t) = e^{-\gamma(t-(2b+t_0))}$. Then, by the explicit evaluation of the integrals, we get

$$g(T) = \begin{cases} 0 & \text{for } t_0 + \dfrac{b_0}{2} \le T < 2b + t_0, \\ \dfrac{4}{b_0}(2s(T) - 1) & \text{for } 2b + t_0 < T < 2b + t_0 + \dfrac{b_0}{2}, \\ -\dfrac{8}{b_0}s(T)(e^{\gamma\frac{b_0}{2}} - 1) & \text{for } 2b + t_0 + \dfrac{b_0}{2} < T \le 3b. \end{cases} \tag{3.6}$$

The function g is not defined at $T = 2b + t_0$ and $T = 2b + t_0 + \frac{b_0}{2}$, where it exhibits discontinuities due to the jumps of the (weak) derivative of φ_T. In particular, at $T = 2b + t_0$ we have

$$g(2b + t_0)^- = 0, \quad g(2b + t_0)^+ = \frac{4}{b_0}.$$

Then g decreases until reaching the second discontinuity at $T = 2b + t_0 + \frac{b_0}{2}$, where

$$g\Big(2b + t_0 + \frac{b_0}{2}\Big)^- = \frac{4}{b_0}(2e^{-\gamma b_0/2} - 1), \quad g\Big(2b + t_0 + \frac{b_0}{2}\Big)^+ = -\frac{8}{b_0}(1 - e^{-\gamma b_0/2}) < 0.$$

Finally, g increases, still remaining negative for larger T (see Figure 2 for an example).

Notice that either the abscissa $2b + t_0$ or $2b + t_0 + \frac{b_0}{2}$ of the points of discontinuity *uniquely* determines the length b.

Now, in order to determine γ it is convenient to *extend g to a right-continuous function* (still denoted by g) for $T \in [0, 3b)$, that is,

$$g(2b + t_0) = g(2b + t_0)^+, \quad g\Big(2b + t_0 + \frac{b_0}{2}\Big) = g\Big(2b + t_0 + \frac{b_0}{2}\Big)^+. \tag{3.7}$$

Then $g(T)$ assumes *maximum value* $g(2b + t_0) = \frac{4}{b_0}$ and *minimum value*

$$g\Big(2b + t_0 + \frac{b_0}{2}\Big) = -\frac{8}{b_0}(1 - e^{-\gamma b_0/2}) := -\Delta. \tag{3.8}$$

The maximum is independent of the unknowns b and γ (and equals the jump at both discontinuities, see Figure 2), while the minimum depends only on γ, so that γ can be uniquely determined as

$$\gamma = -\frac{2}{b_0}\ln\Big(1 - \frac{\Delta b_0}{8}\Big). \tag{3.9}$$

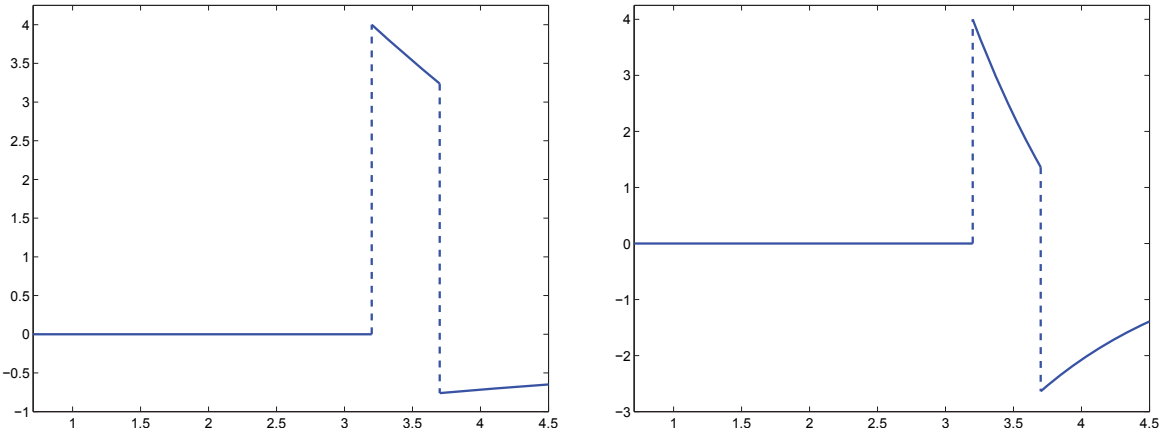

Figure 2: Plot of g for $b_0 = 1$, $b = 1.5$, $t_0 = 0.2$, $\gamma = 0.2$ (left) and $\gamma = 0.8$ (right).

Note that Δ is also equal to the value of the gap

$$g(2b + t_0) - g\Big(2b + t_0 + \frac{b_0}{2}\Big)^- = \frac{8}{b_0}(1 - e^{-\gamma\frac{b_0}{2}}).$$

We can sum up the previous discussion in the following proposition.

Proposition 3.2. *Let $u(x, t)$ be the weak solution to (1.1) with Dirichlet data $u(0, t) = \delta(t - t_0)$ in the sense of (3.3). Assume that the endpoint b and the parameter γ in (1.1) satisfy $b \geq b_0 > 0$ and $\gamma \geq 0$, and that $0 < t_0 < \frac{b_0}{2}$. Moreover, let g be the right-continuous function defined by (3.5)–(3.7). Then, denoting by T_M the abscissa of the unique maximum of g, we have*

$$b = \frac{1}{2}(T_M - t_0). \tag{3.10}$$

Furthermore, the parameter γ is determined by

$$\gamma = -\frac{2}{b_0}\ln\Big(1 + \frac{g_m b_0}{8}\Big), \tag{3.11}$$

where $g_m = g(T_M + \frac{b_0}{2})$ is the minimum value of g.

According to this proposition, the unknown pair (b, γ) is recovered by evaluating the weighted integrals (3.5) of the output flux up to the time $T_M + \frac{b_0}{2}$.

Remark 3.3. If an upper bound $b < \bar{b}$ is known a priori, the flux could be evaluated up to a maximum time $T = 2\bar{b} + t_0 + \frac{b_0}{2}$.

Notice that the value of γ is determined regardless of b. This property could be exploited to improve the evaluation of b. For this, let us suppose that the points of discontinuity are known to lie in the interval $(\overline{T} - \epsilon, \overline{T} + \epsilon)$ and $(\overline{T} + \frac{b_0}{2} - \epsilon, \overline{T} + \frac{b_0}{2} + \epsilon)$, respectively, where $0 < \epsilon < \frac{b_0}{4}$ (this means that $\frac{1}{2}(\overline{T} - t_0 - \epsilon) < b < \frac{1}{2}(\overline{T} - t_0 + \epsilon)$). Then, after computing γ as in (3.9), choose

$$T_M \in \Big(\overline{T} + \epsilon, \overline{T} + \frac{b_0}{2} - \epsilon\Big)$$

and measure the value $g(T_M)$. Since T_M lies between the points of discontinuity, by (3.6) we readily obtain

$$b = \frac{1}{2}(T_M - t_0) + \frac{1}{2\gamma}\ln\Big[\frac{1}{2} + \frac{b_0}{8}g(T_M)\Big].$$

The above formula could be used to provide a better estimate of b provided that γ and $g(T_M)$ are determined with sufficient precision (see below).

Remark 3.4 (The case of the Neumann condition). It is interesting to consider the case $\gamma = 0$ in (1.1), that is, to uniquely determine b when the homogeneous Neumann condition $u_x(b, t) = 0$ is assigned. By setting $\gamma = 0$ in (3.6), it turns out that

$$g(T) = \frac{4}{b_0}\mathbf{1}_{(2b+t_0, 2b+t_0+\frac{b_0}{2})},$$

so that the unknown b is determined by locating the discontinuities of g, which degenerates in a rectangle function.

Remark 3.5. One could also choose any scaled version $m\varphi_T$ of the test function in (3.4), with $m > 0$. In such a case, the function g scales accordingly, while (3.9) still holds with Δ defined by (3.8).

3.1 Stability analysis

We have shown that if u is the solution of (1.1) with impulsive Dirichlet data at $x = 0$, then the function g defined in Proposition 3.2 uniquely determines the parameters (b, γ). We now discuss the stability of such reconstruction procedure. Hence, we will estimate the distance between two points in the plane (b, γ) in terms of some suitably defined distance between two functions g. To this end, notice the following facts:

- By (3.11), the parameter γ is uniquely determined by the minimum value of g.
- By extending $g(T)$ to zero outside the interval $(t_0 + \frac{b_0}{2}, 3b)$, the graphs of two functions with the same γ and $b = b_1$, $b = b_2$ differ by a shift of $b_2 - b_1$ along the T axis.

Let us now define $g_{\{b,\gamma\}} : \mathbb{R} \to \mathbb{R}$ to be the extension to zero of $g(T)$ given by (3.6). For any $b \geq b_0 > 0$ and $\gamma \geq 0$, the function $g_{\{b,\gamma\}}$ is bounded and compactly supported.

Thanks to the two previous remarks, we define the distance

$$d(g_{\{b_1,\gamma_1\}}, g_{\{b_2,\gamma_2\}}) := \int_{\mathbb{R}} |g_{\{b_1,\gamma_1\}}(T) - g_{\{b_2,\gamma_2\}}(T)|\, dT + \left|\inf_T g_{\{b_1,\gamma_1\}}(T) - \inf_T g_{\{b_2,\gamma_2\}}(T)\right|,$$

where the right-hand side is well defined in the set $G \times G$, where

$$G := \{g_{\{b,\gamma\}} : (b, \gamma) \in [b_0, +\infty) \times [0, +\infty)\}.$$

Then we prove the following stability result.

Theorem 3.6. *Let $g_{\{b,\gamma\}}$ be defined as above and assume that $b \geq b_0 > 0$ and $0 \leq \gamma \leq \bar{\gamma}$ for some $\bar{\gamma} > 0$. Then there exist positive constants C and η depending only on b_0 and $\bar{\gamma}$ such that*

$$d(g_{\{b_1,\gamma_1\}}, g_{\{b_2,\gamma_2\}}) \geq C(|b_1 - b_2| + |\gamma_1 - \gamma_2|) \tag{3.12}$$

whenever $|b_1 - b_2| \leq \eta$.

Proof. Let Δ_1, Δ_2 be defined as in (3.8) for $\gamma = \gamma_1$ and $\gamma = \gamma_2$, respectively. By (3.9) and simple calculus, we have

$$|\gamma_1 - \gamma_2| = \frac{2}{8 - b_0\tilde{\Delta}}|\Delta_1 - \Delta_2|,$$

where $\Delta_1 < \tilde{\Delta} < \Delta_2$. By (3.8) and exploiting the bound on γ, we obtain $\tilde{\Delta} \leq \bar{\Delta} < \frac{8}{b_0}$, with $\bar{\Delta}$ as in (3.8) for $\gamma = \bar{\gamma}$, so that

$$|\gamma_1 - \gamma_2| \leq \frac{2}{8 - b_0\bar{\Delta}}|\Delta_1 - \Delta_2|. \tag{3.13}$$

Suppose now that $b_1 < b_2 \leq b_1 + \frac{b_0}{4}$, and consider the function $g_1 - g_2$, where we set $g_1 = g_{\{b_1,\gamma_1\}}$ and $g_2 = g_{\{b_2,\gamma_2\}}$. Note that in the interval $2b_1 + t_0 \leq T < 2b_2 + t_0$ one has

$$g_1(T) = \frac{4}{b_0}(2e^{-\gamma_1(T-(2b_1+t_0))} - 1) \quad \text{and} \quad g_2(T) = 0.$$

Figure 3: Degrees of freedom and nodes associated with the space U_σ^r for $r = 4$.

Moreover, g_1 is decreasing in $2b_1 + t_0 \le T < 2b_2 + t_0$, with

$$g_1(2b_2 + t_0) = \frac{4}{b_0}\left(2e^{-2\gamma_1(b_2-b_1)} - 1\right) \ge \frac{4}{b_0}\left(2e^{-2\bar{\gamma}(b_2-b_1)} - 1\right).$$

The last term is positive provided that

$$b_2 - b_1 < \frac{1}{2\bar{\gamma}} \ln 2.$$

Hence, by defining

$$\eta := \min\left\{\frac{b_0}{4}, \frac{\ln 2}{2\bar{\gamma}}\right\},$$

for $|b_1 - b_2| < \eta$ holds

$$\int_{\mathbb{R}} |g_1(T) - g_2(T)|\, dT > \int_{2b_1+t_0}^{2b_2+t_0} |g_1(T)|\, dT \ge \frac{8K}{b_0}|b_1 - b_2|, \tag{3.14}$$

where the positive constant K depends only on $\bar{\gamma}$ and η. By recalling that $\Delta_i = -\inf_T g_i(T)$ with $i = 1, 2$, result (3.12) follows by estimates (3.13) and (3.14) and by choosing $C = \min\{\frac{8K}{b_0}, (8 - b_0\bar{\Delta})/2\}$. □

4 The discrete problem

The aim of this section is to apply the reconstruction procedure in Proposition 3.2. For this purpose, we compute a numerical approximation of g on a finite number of time levels, thus simulating the actual experimental setting. In particular, to determine T_M (and analogously g_m) it suffices to process all of these values and then use formulas (3.10) and (3.11) to recover the pair (b, γ).

Additionally, to be more realistic with respect to an actual experimental procedure, we also consider the effects of replacing the idealized impulsive stimulus with a Gaussian source as well as of a random noise added to the observed data. Moreover, also the numerical scheme used to solve (1.1) unavoidably introduces a discretization error, which can be assimilated to some further uncertainties in the actual physical setting. Clearly, these error sources cannot be analytically accounted for in an easy way, so that a numerical simulation turns out to be a practical and effective way to asses the performance of the reconstruction procedure under more realistic conditions.

We consider the discretization of problem (1.1). In particular, since we are dealing with a space-time problem, we first discretize in space via a finite element scheme, and then in time by resorting to the Newmark method.

Let us start by subdividing the domain $[0, b]$ into N uniform sub-intervals via the $N + 1$ nodes $\{x_i\}_{i=0}^N$, with $x_{i+1} = x_i + \sigma$, with $\sigma = \frac{b}{N}$, $x_0 = 0$ and $x_N = b$. With a view to the finite element approximation, we introduce the finite-dimensional space

$$U_\sigma^r = \{w \in C^0([0, b]) : w|_{[x_i, x_{i+1}]} \in \mathbb{P}^r\}$$

of piecewise continuous function of degree r, whose corresponding degrees of freedom are denoted by ξ_j, $j = 0, \dots, rN$, following the ordering described in Figure 3.

Thus, the semi-discrete finite element approximation is as follows: for all $t > 0$, find $u^\sigma(t) \in U_\sigma^r$ such that, for all $v^\sigma \in V_\sigma^r$,

$$\int_0^b u_{tt}^\sigma(x, t)v^\sigma(x)\, dx + \int_0^b u_x^\sigma(x, t)v_x^\sigma(x)\, dx + \gamma u^\sigma(b, t)v^\sigma(b) = 0, \tag{4.1}$$

with $u^\sigma(0,t) = h(t)$ and $u^\sigma(x,0) = u_t^\sigma(x,0) = 0$, and where $V_\sigma^r = \{w \in U_\sigma^r : w(0,t) = 0 \text{ for all } t > 0\}$. Notice also that we adopt the standard convention of omitting the dependence on x when, at a given time, functions are meant in U_σ^r.

The algebraic counterpart of (4.1) is provided by the following system of ordinary differential equations:

$$\begin{cases} \widetilde{M}\tilde{\mathbf{u}}_{tt}(t) + \widetilde{K}\tilde{\mathbf{u}}(t) = \mathbf{0}, \quad t > 0, \\ \tilde{\mathbf{u}}(0) = \mathbf{0} \\ \tilde{\mathbf{u}}_t(0) = \mathbf{0}, \end{cases} \tag{4.2}$$

with

$$\tilde{\mathbf{u}}(t) = \{u^\sigma(\xi_i,t)\}_{i=0}^{rN} \in \mathbb{R}^{rN+1}, \quad \widetilde{M} = [\tilde{m}_{ij}]_{i,j=0}^{rN} \in \mathbb{R}^{(rN+1)\times(rN+1)}, \quad \widetilde{K} = [\tilde{k}_{ij}]_{i,j=0}^{rN} \in \mathbb{R}^{(rN+1)\times(rN+1)},$$

with

$$\tilde{m}_{ij} = \int_0^b \phi_i(x)\phi_j(x)\,dx, \quad \tilde{k}_{ij} = \int_0^b \phi_{i,x}(x)\phi_{j,x}(x)\,dx + \gamma\delta_{i,rN}\delta_{j,rN},$$

being the elements of the mass and of the stiffness matrix, respectively, $\delta_{k,rN}$ being the Kronecker symbol, $u^\sigma(\xi_0,t) = h(t)$, and with $\{\phi_k\}_{k=0}^{rN}$ being the finite element basis functions, assumed to be Lagrangian, so that

$$u^\sigma(x,t) = \sum_{k=0}^{rN} u^\sigma(\xi_k,t)\phi_k(x).$$

System (4.2) can be reduced in dimension in order to highlight the known quantities as

$$\begin{cases} M\mathbf{u}_{tt}(t) + K\mathbf{u}(t) = -(h(t)\mathbf{f} + h_{tt}(t)\mathbf{m}) =: \mathbf{F}(t), \quad t > 0, \\ \mathbf{u}(0) = \mathbf{0}, \\ \mathbf{u}_t(0) = \mathbf{0}, \end{cases} \tag{4.3}$$

where[1]

$$\begin{aligned} K &= \widetilde{K}(2 : rN+1, 2 : rN+1) \in \mathbb{R}^{rN\times rN}, \\ M &= \widetilde{M}(2 : rN+1, 2 : rN+1) \in \mathbb{R}^{rN\times rN}, \\ \mathbf{f} &= \widetilde{K}(2 : rN+1, 1) \in \mathbb{R}^{rN}, \\ \mathbf{m} &= \widetilde{M}(2 : rN+1, 1) \in \mathbb{R}^{rN}, \\ \mathbf{u}(t) &= \{u^\sigma(\xi_i,t)\}_{i=1}^{rN} \in \mathbb{R}^{rN}. \end{aligned}$$

Notice that both M and K are symmetric positive definite.

Concerning the time discretization, we focus on the time window $[0,t_f]$ for some final time $t_f > 0$, and divide such interval in N_τ sub-intervals, identified by the time step $\tau = t_f/N_\tau$, such that $t^{n+1} = t^n + \tau$ for $n = 0,\dots,N_\tau - 1$. Then we resort to the Newmark method [10], and in particular to its a-form implementation. This is a well-known one-step algorithm for a second-order ordinary differential system in time describing general damped/undamped structural dynamics applications [4]. In this method, system (4.3) is reformulated in terms of three unknowns, $\mathbf{a} = \mathbf{u}_{tt}$, $\mathbf{v} = \mathbf{u}_t$ and $\mathbf{u}$, so that it becomes

$$\begin{cases} M\mathbf{a}(t) + K\mathbf{u}(t) = \mathbf{F}(t), \quad t \in (0,t_f], \\ \mathbf{u}(0) = \mathbf{0}, \\ \mathbf{v}(0) = \mathbf{0}. \end{cases} \tag{4.4}$$

Then the first equation of (4.4) is evaluated at the time level t^{n+1} as

$$M\mathbf{a}^{n+1} + K\mathbf{u}^{n+1} = \mathbf{F}^{n+1},$$

1 We adopt a standard Matlab syntax to extract array components.

where the superscripts indicate the corresponding time level, supplemented with the following Taylor-like expansions to link the unknowns at t^n and at t^{n+1}:

$$\mathbf{u}^{n+1} = \underbrace{\mathbf{u}^n + \tau\mathbf{v}^n + \tau^2\Big(\Big(\frac{1}{2} - \beta\Big)\mathbf{a}^n}_{\mathbf{u}_p^n} + \beta\mathbf{a}^{n+1}\Big) = \mathbf{u}_p^n + \tau^2\beta\mathbf{a}^{n+1},$$
$$\mathbf{v}^{n+1} = \underbrace{\mathbf{v}^n + \tau((1-\alpha)\mathbf{a}^n}_{\mathbf{v}_p^n} + \alpha\mathbf{a}^{n+1}) = \mathbf{v}_p^n + \tau\alpha\mathbf{a}^{n+1}.$$

The variables $\mathbf{u}_p^n$ and $\mathbf{v}_p^n$ denote *predicted* values for the displacement and the velocity, respectively, and can be computed explicitly since they depend just on the state at time level n. The Newmark one-step procedure to advance in time consists of, given $[\mathbf{u}^n, \mathbf{v}^n, \mathbf{a}^n]$, computing $[\mathbf{u}^{n+1}, \mathbf{v}^{n+1}, \mathbf{a}^{n+1}]$ by the following steps:

$$\begin{aligned}
\mathbf{u}_p^n &= \mathbf{u}^n + \tau\mathbf{v}^n + \tau^2\Big(\frac{1}{2} - \beta\Big)\mathbf{a}^n,\\
\mathbf{v}_p^n &= \mathbf{v}^n + \tau(1-\alpha)\mathbf{a}^n,\\
(M + \tau^2\beta K)\mathbf{a}^{n+1} &= \mathbf{F}^{n+1} - K\mathbf{u}_p^n,\\
\mathbf{u}^{n+1} &= \mathbf{u}_p^n + \tau^2\beta\mathbf{a}^{n+1},\\
\mathbf{v}^{n+1} &= \mathbf{v}_p^n + \tau\alpha\mathbf{a}^{n+1},
\end{aligned}$$

where the first two and the last two assignments are straightforward vector updates. The third line involves solving an algebraic linear system for the unknown $\mathbf{a}^{n+1}$, with a symmetric positive definite matrix being a linear combination of the stiffness and mass matrix.

After dealing with the approximation to the wave equation, we have to address the recovery of the model parameters b and γ by a suitable identification procedure. We summarize the overall algorithm, comprising both the approximation of the wave equation and the estimate of b and γ, in Algorithm 1.

Some remarks are in order. The function in line 2 (and its corresponding second-order derivative in time in line 3) replaces the impulse in (3.1). This is a user-defined Gaussian function, centered at $t = t_0$, with variance λ and with unit integral over $\mathbb{R}$.

The vector function $\mathbf{F}$ in line 4 coincides with definition (4.3).

In lines 5–7, according to a standard finite element approach, we introduce the local degrees of freedom (the $r+1$ uniform nodes associated with the space $\mathbb{P}^r$) on the reference unit interval and form the corresponding global stiffness and mass matrices by typical local-to-global assembly procedures [14]. The relation $\tau = 0.1\sigma$ reduces the dispersion error in the Newmark method.

The time marching process is carried out in lines 11–16, via the Newmark method, after the initialization in lines 8–9.

To compute $g(T)$ in (3.5) we resort to a numerical integration formula after replacing $u_x(0, t)$ with a suitable approximation. Concerning this last issue, the idea is to first interpolate the values $\{\tilde{\mathbf{u}}_k^{n+1}\}_{k=0}^r$ at the generic time level $n+1$ at the $r+1$ uniform nodes $\{\xi_k\}_{k=0}^r$ on the leftmost interval $[0, x_1]$ by a polynomial in $\mathbb{P}^r$. However, for numerical conditioning issues, this approximation is carried out on the reference element: Given $\{(\hat{x}_k, \tilde{\mathbf{u}}_k^{n+1})\}_{k=0}^r$, find the coefficients $\{c_k\}_{k=0}^r$ such that

$$p^r(\hat{x}_j) = \sum_{k=0}^{r} c_k \hat{x}_k^{r-k} = \tilde{\mathbf{u}}_j, \quad j = 0, \dots, r.$$

The coefficients $\{d_k\}_{k=0}^r$ of the polynomial $q^r(x) = \sum_{k=0}^r d_k x^{r-k}$ on the physical interval $[0, x_1]$ are computed by the transformation $\{d_k\}_{k=0}^r = \{c_k\sigma^{k-r}\}_{k=0}^r$. Finally, the approximation w^{n+1} to $u_x(0, t^{n+1})$ is computed in line 17 as

$$w^{n+1} = q_x^r(0) = d_{r-1}, \tag{4.5}$$

with

$$q_x^r(x) = \sum_{k=0}^{r-1} (r-k) d_k x^{r-k-1}.$$

Algorithm 1. The Newmark method and the reconstruction procedure.

1. Input: $b_0, t_0, \lambda, \gamma, b, r, N, t_f, \beta, \alpha$.
2. Define: $h(t) = 1/(\sqrt{2\pi}\lambda)\exp((-(t-t_0)^2)/(2\lambda^2))$.
3. Define: $h_{tt}(t) = ((t-t_0)^2 - \lambda^2)/\lambda^4 h(t)$.
4. Define: $\mathbf{F}(t) = -(h(t)\mathbf{f} + h_{tt}(t)\mathbf{m})$.
5. Define: $\{\hat{x}_k\}_{k=0}^r : \hat{x}_k = \frac{k}{r}$.
6. Set: $\sigma = \frac{b}{N},\ \tau = 0.1\sigma,\ N_\tau = t_f/\tau$.
7. Assemble: $M,\ K$ as in (4.3).
8. Set: $n = 0,\ t^0 = 0,\ \mathbf{u}^0 = \mathbf{v}^0 = \mathbf{0},\ w^0 = 0$.
9. Solve for $\mathbf{a}^0$: $M\mathbf{a}^0 = \mathbf{F}(0)$.
10. For $n = 0 : N_\tau - 1$

    % Newmark step.

    11. $t^{n+1} = t^n + \tau$.
    12. Set: $\mathbf{u}_p^n = \mathbf{u}^n + \tau\mathbf{v}^n + \tau^2(\frac{1}{2} - \beta)\mathbf{a}^n$.
    13. Set: $\mathbf{v}_p^n = \mathbf{v}^n + \tau(1-\alpha)\mathbf{a}^n$.
    14. Solve for $\mathbf{a}^{n+1}$: $(M + \tau^2\beta K)\mathbf{a}^{n+1} = \mathbf{F}^{n+1} - K\mathbf{u}_p^n$.
    15. Set: $\mathbf{u}^{n+1} = \mathbf{u}_p^n + \tau^2\beta\mathbf{a}^{n+1}$.
    16. Set: $\mathbf{v}^{n+1} = \mathbf{v}_p^n + \tau\alpha\mathbf{a}^{n+1}$.

    % Approximation to $u_x(0, t^{n+1})$.

    17. Compute: w^{n+1} by (4.5).
18. End.

% Estimate of b, γ.

19. Compute: $g(T^n)$ by (4.6) for $T^n \in [\frac{b_0}{2} + t_0, 3b - \tau]$.
20. Compute: b by (4.7).
21. Compute: $\Delta = -\min_n g(T^n)$.
22. Compute: γ by (3.9).

As for the numerical integration involved in (3.5), we consider the interval $[\frac{b_0}{2} + t_0, 3b - \tau]$ for T, and sample this interval with the same step used for the Newmark method, i.e., τ, and denote by T^n the variable right endpoint in the integral in (3.5). Additionally, we resort to a composite quadrature rule based on the uniform nodes $\{t^n\}_{n\geq 0}$. Thus, we divide the interval $[0, T^n]$ in $N_n = T^n/\tau$ sub-intervals, and employ the composite trapezoidal quadrature rule, taking into account that $w^0 = 0$, due to the initial condition in (1.1). This yields the computation in line 19:

$$g(T^n) \simeq \tau \sum_{k=1}^{N_n - 1} w^k \varphi_{T^n}(t^k) + 0.5\tau w^{N_n}\varphi_{T^n}(t^{N_n}). \tag{4.6}$$

We are now ready to compute the pair (b, γ) in lines 20–22, inspired by (3.10) and (3.11). In particular, b is derived by computing first $T_M = \arg\max_n \frac{dg}{dT}(T^n)$ in a neighborhood of the positive steep gradient of g, and then the quantity

$$b = 0.5(T_M - t_0). \tag{4.7}$$

As for γ, we exploit (3.9) after properly approximating Δ in (3.8) as the minimum of $g(T^n)$ over the interval $[\frac{b_0}{2} + t_0, 3b - \tau]$ up to the sign.

A numerical assessment. We now carry out two numerical experiments, corresponding to the data in Figure 2. Concerning the configuration on the left, we pick the input parameters to Algorithm 1: $b_0 = 1$, $t_0 = 0.2$, $\lambda = 0.0025$, $\gamma = 0.2$, $b = 1.5$, $r = 2$, $N = 6000$, $t_f = 3b + 2t_0 = 4.7$, $\beta = \frac{1}{4}$ and $\alpha = \frac{1}{2}$. For estimating b, we consider the plot of g in Figure 4 (left), and zoom in on around the first discontinuity in Figure 4 (center). With high confidence, we can state that $3.19 < 2b + t_0 < 3.21$. The derivative of $g(T)$, represented in this interval in Figure 4 (right), predicts $T_M = 3.200075$, from which we can recover the value $b = 1.5000375$, which is a very accurate approximation to the exact value.

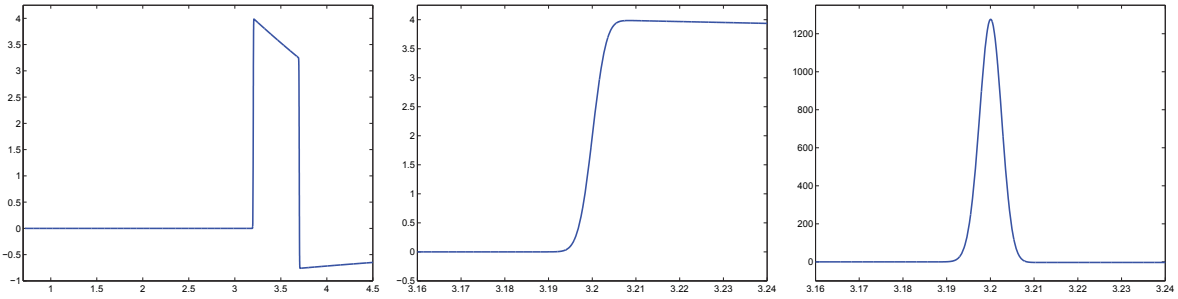

Figure 4: Test 1: Plot of $g(T^n)$ (left), of a detail (center) and of $\frac{dg}{dT}(T^n)$ (right) for $T^n \in [3.16, 3.24]$.

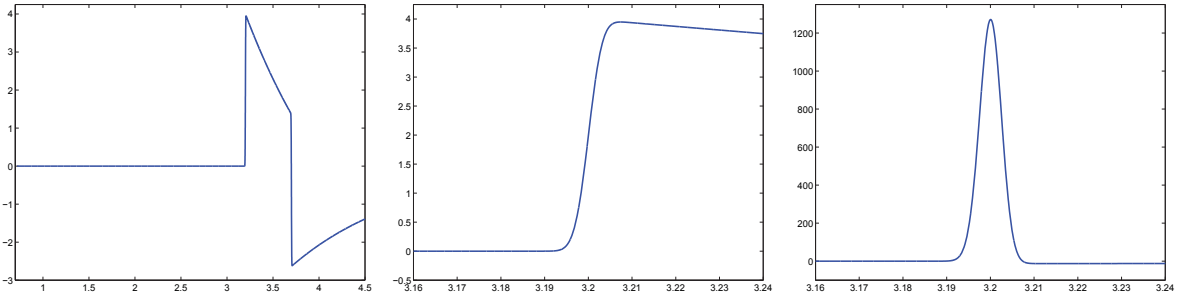

Figure 5: Test 2: Plot of $g(T^n)$ (left), of a detail (center) and of $\frac{dg}{dT}(T^n)$ (right) for $T^n \in [3.16, 3.24]$.

SNR	T_M	b	γ
70	3.200099	1.5000498	0.199854
60	3.200140	1.5000700	0.200574
50	3.199943	1.4999717	0.203104

Table 1: Test 1 with noisy data: reconstructed quantities for three different values of SNR.

The computed value in line 21, based on Figure 4 (left), is $\Delta = 0.759734$, which yields the estimated value $\gamma = 0.199567$, very close to the exact value, differing only by circa 0.2 % with respect to a relative error.

Figure 5 collects the results associated with the configuration on the right in Figure 2. The same parameters as in the previous case are chosen, except for γ set to 0.8. The estimated values of the parameters are $T_M = 3.200050$, $b = 1.5000250$, $\Delta = -2.618865$ and $\gamma = 0.793084$, with a relative error on this latter of about 0.8 %.

We now consider the more realistic case of a noisy signal, i.e., we suppose that additive noise affects the measurement, so that the actual observed data is $\widetilde{g} = g + w_n$, where w_n represents noise. In particular, we assume w_n to be an independent and identically distributed random variable according to a Gaussian density function $\mathcal{N}(0, s_d)$ characterized by a zero mean and a standard deviation s_d. This latter depends on the signal-to-noise ratio SNR with respect to the power of the signal in the following way: Let $v \in \mathbb{R}^m$ be a generic discrete signal sampled at m time levels. Then its power $E(v)$ can be defined as $\|v\|^2/m$, with $\|\cdot\|$ being the Euclidean norm in $\mathbb{R}^m$. Denoting by $\mathrm{snr} = 10^{\mathrm{SNR}/10}$ the signal-to-noise ratio in linear scale, we have that the standard deviation is $s_d = \sqrt{E(v)/\mathrm{snr}}$. In practice, Algorithm 1 is applied also to the noisy case by replacing the function g in lines 19–22 with the noisy data $\widetilde{g}$ obtained by the Matlab command `awgn(g,SNR,'measured')` which performs automatically the procedure just described. We consider the same setting as in the first test case, and select the values 50, 60 and 70 of SNR and, due to the randomness of the noise, we determine the estimate of the parameters b and γ by averaging the results over 50 samples of w_n.

Figure 6 shows details of the function g and of its derivative for above choices of SNR.

As expected, differentiating a noisy function emphasizes the noise level. However, the peaks are still detectable. The quantitative results of the reconstruction procedure are gathered in Table 1.

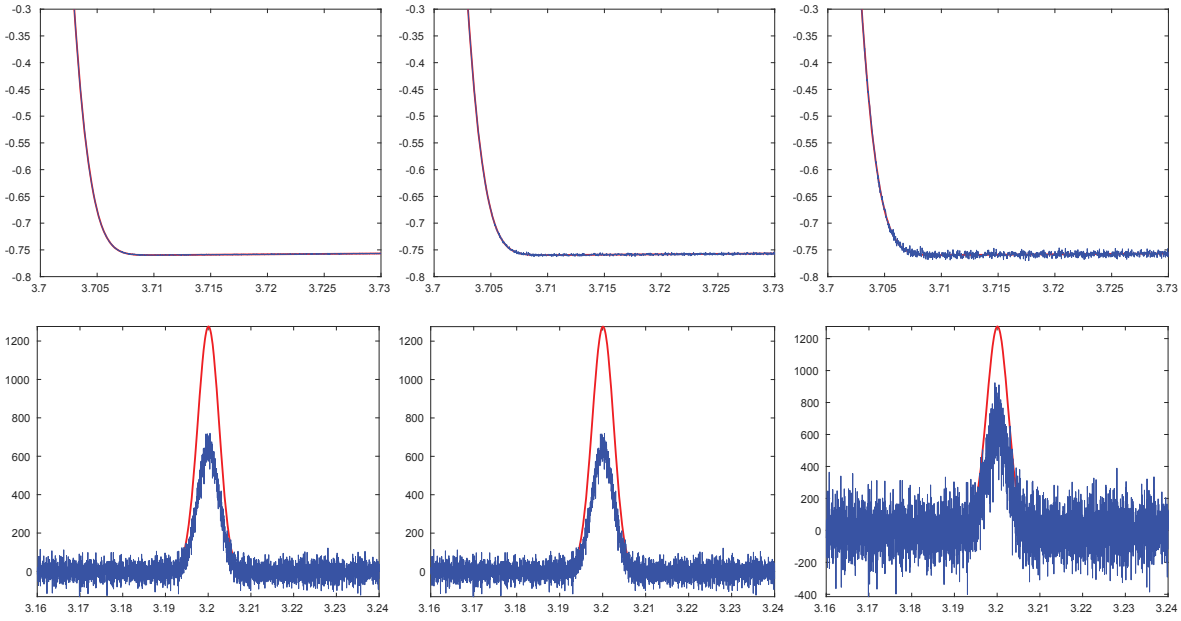

Figure 6: Test 1 with noisy data: Plot of $g(T^n)$ (top) and of $\frac{dg}{dT}(T^n)$ (bottom) for $T^n \in [3.7, 3.73]$ and $T^n \in [3.16, 3.24]$, respectively, for SNR = 70 (left), 60 (center) and 50 (right).

In the worst case, SNR = 50, the relative error on γ turns out to be 1.6 %, thus assessing the good robustness of the proposed reconstruction procedure. For this test case, the value 50 represents somewhat the minimum SNR which can be dealt with by the reconstruction procedure, as is. Indeed, for smaller values of the SNR the noise present in the numerical derivative of $g(T)$ is of the same order of magnitude as the main spikes, so that it is no longer possible to easily detect the abscissa T_M. On the other hand, in a real situation, in the presence of a stronger noise it is possible to apply a suitable filter to obtain a derivative of g enjoying the same amount of noise as that acting on g, and then to follow the same steps in lines 19–22 of Algorithm 1. Due to the extra technical details involved, we will not address this issue. Moreover, the reconstruction procedure is not affected considerably and remains as effective and stable as with the moderate values of noise just considered in Table 1.

5 Conclusions

The exact solvability of the linear wave equation in a one-dimensional setting turns out to be a non-trivial issue when the spatial interval is bounded and mixed-boundary conditions complete the problem. In particular, the Robin data makes the problem more challenging with a view to the computation of the solution in closed form. Indeed, the constructive procedure used in the proof to Proposition 2.1, although based on the standard method of characteristics, demands a particular care due to the boundedness of the spatial domain. In principle, we can extend the solution to larger times, though the technicalities become more involved.

The reconstruction formulas (3.10) and (3.11) provide a practical way to compute the unknown parameters. This is corroborated by the numerical investigation in Section 4 which shows that the accuracy of the recovered parameters is high, thus assessing the reliability of Algorithm 1. The regularization of the Dirichlet data (i.e., the replacement of the impulsive signal with a Gaussian function) required by the numerical procedure can be conceived as a possible physical effect due to measurement errors. Nevertheless, this smoothing does not spoil the physics of the problem, thanks to both a stable recovery procedure (as shown in Section 3.1) and a robust numerical scheme (the Newmark finite element method).

Finally, we briefly discuss possible extensions of our reconstruction method to problems with a time dependent γ. For example, it could be interesting to assume that the Robin coefficient decreases exponentially

in time, modeling a transition over time from elastic to a free-force at the boundary. In this case, we could suitably modify the proposed reconstruction procedure taking into account (2.10) in order to identify also the unknown decay rate. We expect to preserve the stability of the reconstruction algorithm also in this case. The case of a non-homogeneous Robin boundary condition, discussed in Remark 2.3, can be dealt with too, e.g., by employing the superposition principle to split the effect of $h(t)$ and $f(t)$ also in the reconstruction procedure.

References

[1] M. J. Crocker, *Handbook of Acoustics*, John Wiley & Sons, New York, 1998.

[2] V. Bacchelli, M. Di Cristo, E. Sinchich and S. Vessella, A parabolic inverse problem with mixed boundary data. Stability estimates for the unknown boundary and impedance, *Trans. Amer. Math. Soc.* **366** (2014), no. 8, 3965–3995.

[3] L. C. Evans, *Partial Differential Equations*, Grad. Stud. Math. 19, American Mathematical Society, Providence, 2010.

[4] T. J. R. Hughes, *The Finite Element Method. Linear Static and Dynamic Finite Element Analysis*, Dover, Minneola, 2000.

[5] S. O. Hussein, D. Lesnic and M. Yamamoto, Reconstruction of space-dependent potential and/or damping coefficients in the wave equation, *Comput. Math. Appl.* **74** (2017), no. 6, 1435–1454.

[6] M. Ikawa, *Hyperbolic Partial Differential Equations and Wave Phenomena*, Transl. Math. Monogr. 189, American Mathematical Society, Providence, 2000.

[7] C. Isakov, On uniqueness of obstacles and boundary conditions from restricted dynamical and scattering data, *Inverse Probl. Imaging* **2** (2008), 151–165.

[8] D. Lesnic, S. O. Hussein and B. T. Johansson, Inverse space-dependent force problems for the wave equation, *J. Comput. Appl. Math.* **306** (2016), 10–39.

[9] S.-W. Na and L. F. Kallivokas, Direct time-domain soil profile reconstruction for one-dimensional semi-infinite domains, *Soil Dyn. Earthq. Eng.* **29** (2009), 1016–1026.

[10] N. M. Newmark, A method of computation for structural dynamics, *J. Eng. Mech. Div.* **3** (1959), 67–94.

[11] A. A. Nikitin, On the mixed problem for the wave equation with the third and first boundary conditions, *Differ. Equ.* **43** (2007), no. 12, 1733–1741.

[12] A. N. Tikhonov and A. A. Samarskii, *Equations of Mathematical Physics*, Dover Publications, New York, 1990.

[13] G. Q. Xie, A new iterative method for solving the coefficient inverse problem of the wave equation, *Comm. Pure Appl. Math.* **39** (1986), 307–322.

[14] O. C. Zienkiewicz, R. L. Taylor and J. Z. Zhu, *The Finite Element Method: Its Basis and Fundamentals*, 7th ed., Elsevier/Butterworth Heinemann, Amsterdam, 2013.